A narrow-band wavelength-tunable laser system delivering high-energy 300 ps pulses in the near-infrared

F. Brandi,[a] I. Velchev, D. Neshev, W. Hogervorst, and W. Ubachs
Laser Centre, Department of Physics and Astronomy, Vrije Universiteit, De Boelelaan 1081, 1081 HV Amsterdam, The Netherlands

(Received 20 May 2002; accepted 30 September 2002)

We report on the operation of a novel laser system delivering high-energy pulses in the near-infrared region. The pulses are nearly Fourier-transform limited (time-bandwidth product of 0.48), providing narrow-band radiation ($\sim$1.5 GHz), with an energy of 225 mJ and 10 Hz repetition rate. The pulse duration of 320 ps covers the intermediate region between *Q*-switched and mode-locked lasers, and provides high peak powers. The nearly Gaussian beam profile, with a beam quality factor of $M^2 = 2.5$, enables tight focusing, reaching intensities exceeding 5×10^{13} W/cm^2. The system operation is demonstrated near 780 nm, however, the tunability extends over the range 700–970 nm. The laser system is suitable for high-order harmonic generation in the extreme-ultraviolet region for high-resolution frequency domain spectroscopy. © *2003 American Institute of Physics.*
[DOI: 10.1063/1.1524714]

I. INTRODUCTION

The majority of modern high peak power pulsed laser sources is based on the concept of *Q* switching and mode locking. The most commonly used *Q*-switched lasers, the Nd:yttritium–aluminum–garnet (YAG) laser and a variety of excimer lasers, generate powerful pulses with typical durations of 5–15 ns. These sources are often employed for pumping secondary, tunable pulsed lasers. Despite the advances in solid state and semiconductor laser technology, dyes in solution are still widely applied as gain media in such tunable lasers. As a consequence of their typical excited state lifetime of about 1 ns, pulsed dye lasers have an excellent trigger stability, with respect to the *Q*-switched laser, within a fraction of the pulse duration. Mode-locked lasers have typical pulse durations below 50 ps. Recent developments utilize Kerr-lens mode locking in Ti:sapphire (Ti:Sa) producing pulses as short as 5 fs. Such radiation sources have a wide range of applications in many areas of science, specifically in high-order harmonic generation and x-ray production.

The present article describes an alternative laser source developed from the point of view achieving narrow-band and tunable extreme ultraviolet (XUV) radiation as a tool for frequency domain spectroscopy. Four-wave mixing with nanosecond laser pulses in gaseous media has become a well-established technique and in the past decade several groups have demonstrated the generation of Fourier-transform (FT) limited nanosecond pulses in the XUV domain with on-line applications in spectroscopy.[1–3] Although Eikema *et al.*[2] succeeded in generating fifth harmonic at wavelengths as short as 58 nm with FT-limited nanosecond pulses, the photon yield remained below 10^5 photons per pulse. Further upscaling of nanosecond pulses towards higher energies, in order to obtain the peak intensities required for efficient fifth and seventh harmonics generation, is hardly feasible. Furthermore, such highly energetic pulses would fully ionize the gaseous medium used for harmonic generation, which would leave no harmonic conversion yield. On the other hand it has been demonstrated that at intensities above 10^{13} W/cm^2 the so-called plateau of high harmonics is reached.[4] Initially, studies on the plateau region were performed with nontunable mode-locked laser pulses at typical durations of 50 ps;[5] meanwhile, with the production of energetic pulses at sub-10 fs durations, harmonics at $n \sim 100$ have been demonstrated.[6] However, such sources have an intrinsically broad frequency spectrum ($\sim$100 nm).

From the perspective of XUV frequency domain spectroscopy with higher resolution than that achievable with synchrotron sources, where the limiting bandwidth is at 1 cm^{-1},[7] the range of intermediate pulse durations between the typical *Q*-switched and mode-locked lasers is of interest. An XUV source with sub-cm^{-1} bandwidth can be developed on the basis of high-order harmonic generation, provided that FT-limited pulses of 100–500 ps duration and peak intensities higher than 5×10^{12} W/cm^2, are produced. One successful approach is that of a distributed feed-back dye laser (DFDL), which in principle produces wavelength-tunable sub-nanosecond pulses with FT-limited bandwidth.[8,9] The tunability of a DFDL system is intrinsically complicated in view of the fact that its wavelength is determined by the creation of a periodic intensity modulation in the gain medium. At the Lund Laser Center, an XUV-laser source was constructed[10] based on harmonic generation using the amplified output of a DFDL system, emitting tunable pulses of about 50 ps duration. Even though the laser pulses at the fundamental wavelength were claimed to be FT limited, the XUV bandwidth was 30 cm^{-1}, more than an order of magnitude beyond the FT limit.[10] This system generates harmonics on the plateau at wavelengths as short as 35 nm and is

[a]Author to whom correspondence should be addressed; electronic mail: brandi@nat.vu.nl

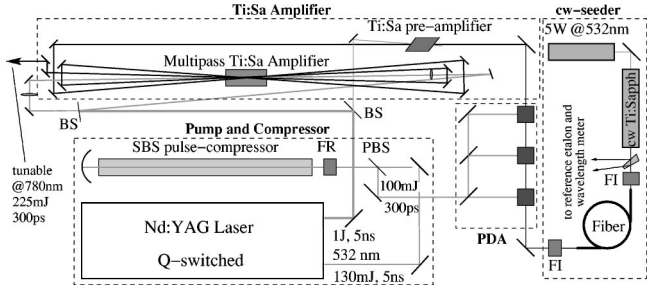

FIG. 1. Schematic diagram of the laser system; FI: Faraday isolator; BS: beam splitter; PBS: polarizing beam splitter; FR: Fresnel Rhomb.

routinely used for spectroscopic investigations.[11]

Our work focuses on an alternative method for producing pulses in this intermediate temporal domain. In a series of studies it has been shown that the FT-limited output of frequency-doubled *Q*-switched Nd:YAG lasers can be temporally compressed from 5–6 ns to 300 ps with conversion efficiencies of 90%, using the stimulated Brillouin scattering (SBS) process in a liquid.[12–14] Here we demonstrate that it is possible to convert fixed-frequency, compressed pulses from a *Q*-switched Nd:YAG laser into wavelength-tunable pulses using a traveling-wave pulsed-dye amplifier (PDA). Near-infrared dyes in solution are used as a gain medium in the PDA. Wavelength-tunable pulses of 300 ps duration are produced and subsequently amplified in a Ti:Sa amplifier, yielding output energies of 225 mJ/pulse at 10 Hz repetition rate. The physical characteristics of this laser system are described in terms of frequency bandwidth, pulse duration, and spatial beam quality. The properties are such, that under focusing conditions, peak intensities higher than 10^{13} W/cm^2 can be produced. Therefore, the pulses produced by the laser system are well suited for future applications involving higher-order harmonic generation in the plateau region, thus providing a potential coherent source of sub-cm^{-1} bandwidth XUV radiation with wavelengths as short as 35 nm.

II. LASER SYSTEM

A schematic diagram of the laser system is shown in Fig. 1. The primary source is a continuous wave (cw) Ti:Sa ring-laser pumped by a solid-state cw laser, delivering narrow-band tunable radiation in the near-infrared (Sec. II A). Its output is transmitted through a short, polarization-maintaining single-mode fiber to seed a three-stage pulse-dye amplifier (Sec. II C), pumped by 300 ps FT-limited pulses from the compressed secondary output of an injection seeded, *Q*-switched and frequency-doubled Nd:YAG laser (Sec. II B). Compression of the pump laser is achieved by stimulated Brillouin scattering in a water cell.[14]

After dye amplification, pulses of ~300 ps duration and energy of 2 mJ are obtained and further amplified in two Ti:Sa crystals pumped by the main frequency-doubled output of the Nd:YAG laser (see Sec. II D). At the output of the amplification chain, nearly FT-limited pulses of 320 ps, with energy of 225 mJ and tunable around 780 nm are produced.

A. cw seeder

The fundamental frequency of the laser system is provided by a cw Ti:Sa ring-laser (Coherent 899-21) pumped by a frequency-doubled diode-pumped Nd:YVO_4 laser (Spectra Physics Millennia 5 W). Wavelengths within the Ti:Sa range are generated with 550 mW power and 1 MHz bandwidth. Continuous single-mode scanning spans up to 30 GHz. While the experiments described here are performed around 780 nm, the tunability of this fundamental seed source covers the range 700–970 nm.

Two auxiliary beams are created from the main laser beam using a glass wedge. One is sent to a wavelength meter (Burleigh WA-20) for on-line absolute frequency monitoring, while the other is sent to a reference etalon for relative frequency measurements.

The laser beam transmitted through the wedge passes through a Faraday isolator and is launched into a short (1 m) polarization-maintaining single-mode fiber (3M FS-PM-4611). The optical isolator ensures that light, reflected from the input tip of the fiber, is not coupled back into the ring laser, thereby disturbing its frequency stabilization. The fiber decouples the alignment of the cw ring laser from that of the PDA hence, increases stability of operation, and additionally serves as spatial filter ensuring a TEM_{00} seed beam. At the output of the fiber, another Faraday isolator is placed to prevent damage of the output tip of the fiber from possible counter-propagating amplified spontaneous emission radiation arising when the PDA is not well seeded, e.g., during the alignment of the pump beams. The light transmitted through the isolators and single mode fiber, typically 250 mW, is used for seeding the three-stage pulse-dye amplifier.

B. Pump and compressor

The pump laser of the system is an injection seeded, *Q*-switched Nd:YAG laser (Quanta Ray GCR-330) operating at 10 Hz repetition rate. The main frequency-doubled output of the Nd:YAG laser delivers 5 ns pulses at 532 nm with an energy of 1 J and is used to pump the Ti:Sa amplifier. The leftover of the fundamental infrared radiation from the Nd:YAG laser is frequency doubled in a second crystal, where pulses of 130 mJ at 532 nm are produced. These pulses are compressed down to 300 ps and used to pump the PDA.

The beam from the secondary output of the Nd:YAG laser passes through a thin-film polarizer used as a high-power polarizing beam splitter (PBS). After a Fresnel rhomb the horizontally polarized beam is transformed into a circular polarization state and enters a Brillouin cell filled with water. A concave mirror, of 10 cm focal length, placed behind the cell focuses the light back into the water. In the focal plane a phase-conjugate backreflected Stokes pulse is generated, which is amplified by stimulated Brillouin scattering along the counter-propagating input pulse. This gives rise to temporal compression towards pulse duration corresponding to the lifetime of acoustic phonons in the liquid. For water at wavelength of 532 nm, the lower limit is 300 ps, which is reached routinely if the pump energies are sufficiently high (for more details on the SBS pulse compression see Ref. 14).

The SBS pulses are separated taking advantage of their polarization. The SBS process does not conjugate the polarization state of the light, hence, after passing through the Fresnel rhomb again, the polarization is orthogonal to the input one and is reflected by the PBS. At the output of the SBS compressor, pulses with energy of 100 mJ are obtained. The Stokes SBS pulses are redshifted by ~ 7 GHz with respect to the pump pulses; this has no effect on the output frequency of the tunable PDA system, since the compressed pulses are only used for creating a population inversion in the gain medium.

C. Pulsed-dye amplifier

A crucial issue for the design of the present laser system is the conversion of the compressed pump pulses into pulses tunable in wavelength and with pulse duration similar to that of the pump. In a setup employing traveling-wave amplification the excited state lifetime of the gain medium must be of the same order or smaller than the pump pulse duration. The excited state lifetime of some near-infrared dyes, for which the gain curves overlap with the Ti:Sa gain curve, are measured by monitoring the fluorescence after femtosecond (100 fs at 530 nm) pulse excitation. The fluorescence signal is recorded with a fluorescence streak camera having temporal resolution better than 3 ps.

The dyes are dissolved in methanol at typical concentrations used in dye lasers, i.e., 100 mg/l (the LDS dyes are obtained from Exciton, whereas the Styryl-9 and Pyridine-2 dyes are obtained from Radiant Dyes). For some dyes, measurements at different concentrations are performed to verify if stimulated emission would reduce the excited state lifetime, but no such effects are found. The possibility to measure dispersed fluorescence by the fluorescence streak camera is employed to verify whether the specific wavelength in the fluorescence channel affects the lifetimes. Such effects are not found except in the case of LDS-925 dissolved in methanol. This liquid emits fluorescence in a window around 925 nm with a typical response of 150 ps, but additionally a minor channel of yellow fluorescence is observed with a decay time of 1–2 ns. This phenomenon is not further investigated. Finally, for the case of LDS-751 dye the dependence of the lifetime on the solvent is studied. With the use of propylene–carbonate the decay time is found 25% longer and with ethanol it is 40% longer than for methanol. The experimentally determined fluorescence decay curves are shown in Fig. 2. The six dyes cover the Ti:Sa gain range from 680 to 970 nm. All investigated near-infrared (IR) dyes exhibit an excited state lifetime of 150–400 ps, hence, they are suitable for producing pulses of 300–400 ps duration in a traveling-wave amplifier setup pumped by the SBS-compressed pulses at 532 nm.

The PDA setup, shown in detail in Fig. 3, consists of three dye cells. The first cell of the amplifier chain (139 mg/l LDS 765 in methanol) is transversely pumped by 4% of the pump power. The emerging pulses are spatially filtered and then amplified in two consecutive amplification cells (39 mg/l), both longitudinally pumped in direction opposite to the seed beam. This design has the advantage that the gain increases along the propagation direction of the seed beam. Such a geometry also reduces the amount of spontaneous emission. The pump beams are focused such that their beam diameters match those of the seed beam in the cells. The

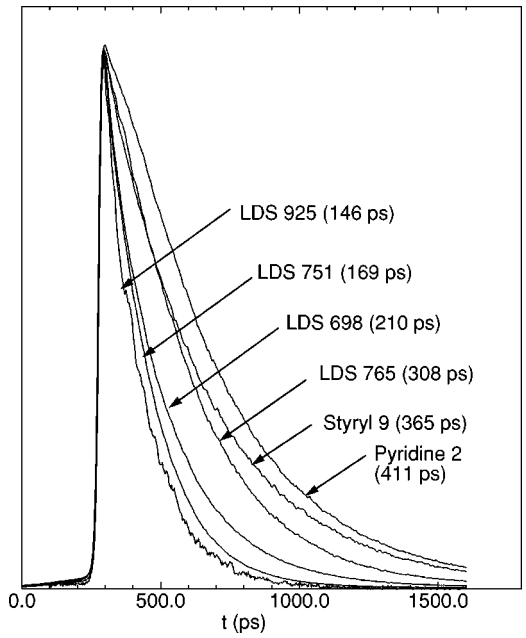

FIG. 2. Fluorescence decay curves for various near-infrared dyes dissolved in methanol at their typical concentrations as used in dye lasers. The measurements were performed by excitation with a femtosecond pump pulse at 530 nm and fluorescence was detected by a picosecond fluorescence streak camera. The experimentally determined decay times are specified for each curve.

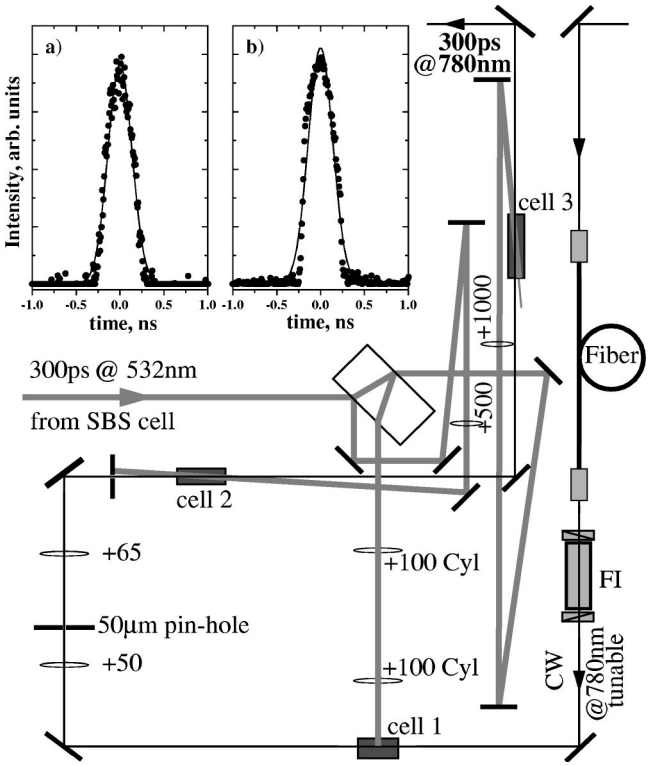

FIG. 3. Detailed scheme of the PDA setup. In the inset the typical temporal profile of the pump pulse (a), FWHM=320(20) ps, and PDA output pulse (b), FWHM=330(20) ps, are shown.

second amplifying cell is pumped by 4% of the pump power, while the remaining 90 mJ pumps the last cell. In the geometrical layout of the PDA special care must be taken to match the timing of the pump and the IR pulse generated in the first cell, in view of the rather short duration of the pulses ($\sim$10 cm spatial length) and the short excited state lifetime of the dye.

In the inset of Fig. 3 the typical temporal profile of the pump pulse (a) and output pulse (b) of the PDA are shown. These measurements are performed using a streak camera (Hadland IMACON 500-20 ps), and result in 320(20) ps full width at half maximum (FWHM) pulse duration for the compressed pumping pulses and 330(20) ps for the PDA output pulses. The alignment of the PDA is optimized on maximum output power, measured at the final output, about 10 m away from the last dye cell. By monitoring the beam in the far field, the contribution of the amplified spontaneous emission is minimized, and a good spatial beam quality is obtained. Typical energy of the PDA output pulses is about 2 mJ, without correcting for the reflection and absorption losses of the Ti:Sa crystals.

D. Ti:sapphire amplifier

The Ti:sapphire amplifier consists of two stages: a single-pass preamplifier followed by a multipass amplifier. The laser beam from the main output (5 ns, 1 J) of the powerful Nd:YAG laser is split into two parts by a 90/10 beam splitter, providing two pump channels of approximately 900 mJ for the multipass amplifier, and 100 mJ for the single-pass preamplifier.

The crystal in the preamplifier is longitudinally pumped and Brewster cut to avoid reflection losses. It is mounted in a brass holder, and the rectangular cross section of the crystal allows for a good direct-contact cooling from four sides. The timing of the pump and seed beams is not so critical as for the PDA. The $\sim 3\ \mu$s lifetime of the Ti:Sa excited state provides enough room for time delay between the seed and pump pulse on a time scale of a few tens of nanoseconds. In the practical realization of the preamplifier the pump pulse arrives 13.6 ns before the seed pulse, as measured with a fast photodiode. Direction and size of the pump beam are optimized to achieve maximum amplification. The typical pulse energy after the preamplifier is $\sim$6 mJ, corresponding to an amplification factor of about 3.

The power amplifier of the laser system is a four pass Ti:Sa amplifier in a monoplanar geometry. The crystal is a high-damage threshold, high-quality laser rod. It has cylindrical shape, with length and diameter of 10 mm. The plane parallel faces are broadband antireflection coated in order to minimize reflection losses, at both pump and seed wavelengths. The crystal holder is a massive brass cylinder. Thermal contact is ensured by a copper cylindrical ring which hosts the crystal and is nested into the brass holder. The holder is temperature stabilized with an active water cooling system and the typical working temperature is 20 °C. The crystal is longitudinally pumped from both sides. The main pump beam is divided with a 50/50 beam splitter into two beams that are focused by two lenses ($f=1$ m) to have diameter at the crystal of about 8 mm. A time delay of $\sim$5 ns is introduced between the two pump pulses in order to avoid their interference inside the crystal. Pulses of 225 mJ are obtained from the four-pass amplifier, corresponding to an amplification factor of about 38.

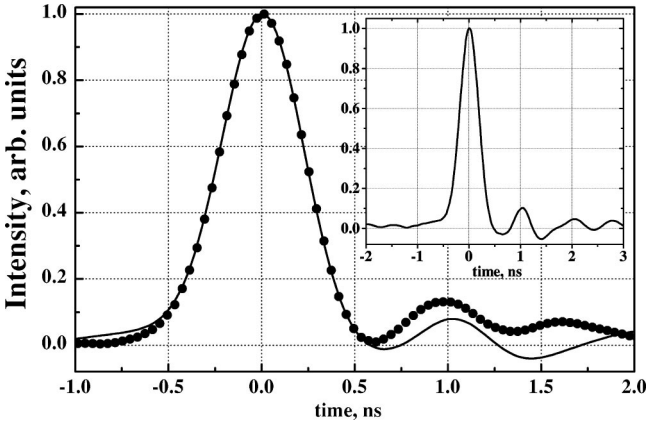

FIG. 4. Measurement of the time duration of the amplified infrared pulses. The dots are the experimental points measured using a fast photodiode and a 1 GHz oscilloscope; the solid line is the convolution of a Gaussian profile (FWHM=300 ps) and the impulse response function of the detection system (shown in the inset).

III. CHARACTERIZATION OF THE LASER SYSTEM

In this section the characteristics of the high-energy output pulses of the laser system are presented. In Sec. III A the pulse time duration and the frequency bandwidth of the pulses are characterized. In Sec. III B the spatial quality of the output beam is evaluated.

A. Temporal and frequency characteristics

The time duration of the pulses is measured with a fast photodiode in combination with a 1 GHz oscilloscope (Tektronix TDS 680B, 5Gs/s). The result of a single shot measurement for a selected short pulse is shown in Fig. 4. The impulse response function (IRF) of the detection system, measured with 100 fs pulses, is also shown in the inset of Fig. 4. Due to the slow response of the detection system a deconvolution procedure is necessary to extract the actual pulse time profile from the measured curve. Assuming Gaussian pulses, the convolution of the IRF and the pulse temporal profile is calculated, with the FWHM of the Gaussian as the only parameter. In Fig. 4, the solid line curve is obtained with a FWHM of 300 ps for the time profile of the pulse. The average pulse duration of the powerful infrared pulses, estimated on the basis of several single shot measurements, is 320(20) ps.

The frequency bandwidth of the pulses is measured using a solid etalon with a free spectral range (FSR) of 21 GHz and finesse 25. The output of the laser system, attenuated using several neutral density filters, is sent through the etalon, while scanning the cw Ti:Sa ring laser. The transmission of the etalon, measured with a fast photodiode in combination with a boxcar integrator, is shown in the lower trace of Fig. 5 (open circles). The transmission through the reference etalon (FSR=7.5 GHz) of the cw light from the ring Ti:Sa

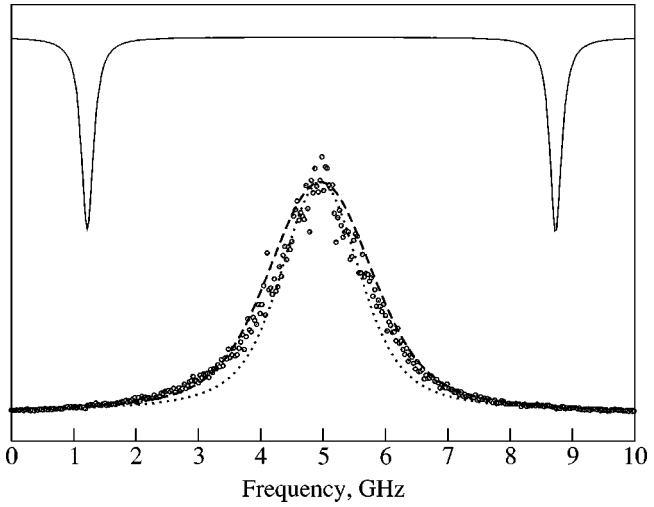

FIG. 5. Spectral bandwidth of the powerful infrared pulses. In the lower part the transmission of the pulses when scanned through a peak of an etalon (FSR=21 GHz) is shown (open circles); the dashed and dotted curves are the convolution of the Airy function with a Gaussian profile with FWHM of 1.8 and 1.2 GHz, respectively. In the upper part the transmission of the seeding light through a reference etalon (FSR=7.5 GHz) is depicted (inverted).

laser (upper trace of Fig. 5) is measured simultaneously, and gives the relative frequency scale. To evaluate the frequency bandwidth of the pulse a Gaussian spectral profile is assumed, and the transmission of the etalon is calculated convoluting the transmittance of the etalon, i.e., the Airy function, with a Gaussian profile with the FWHM as a parameter. The dashed and dotted curves on Fig. 5, are the results of the calculations assuming a FWHM of 1.8 and 1.2 GHz, respectively. The FWHM of the spectral density of the pulse is estimated to be 1.5(3) GHz. The product of the FWHMs of the temporal and spectral profiles of the powerful infrared pulses is about 0.48, hence, demonstrating that the pulses are close to the FT limit (in which case the product is 0.44).

Since the output of the amplified beam is intended for use in high-resolution frequency-domain spectroscopic studies the value of the central frequency of the pulses is of importance. The absolute frequency of the cw-seed laser is accurately measurable by comparison to stabilized etalon fringes and reference standards. The saturated iodine spectrum produces an accuracy of 1 MHZ (1σ).[15,16] Although its use has not yet been established for the entire tuning range of the Ti:Sa laser, the I_2 saturated reference standard can be used up to 830 nm. As it is known from several studies on traveling-wave dye amplifiers, the amplified pulses can undergo a net frequency shift with respect to the seeding light[2,17,18] (chirp shift). The origin of such effect is the time dependence of the gain during the amplification process, and its magnitude depends on the dye used and the wavelength position with respect to the maximum of the dye curve. In high-precision pulsed spectroscopy the chirp shift, typically on the order of 30 MHz in the visible, is the main source of systematic error. In the systems investigated in Refs. 2, 17, and 18 pulse durations were in the range 5–15 ns, and the increased peak intensities in the present system may give rise to larger frequency offsets.

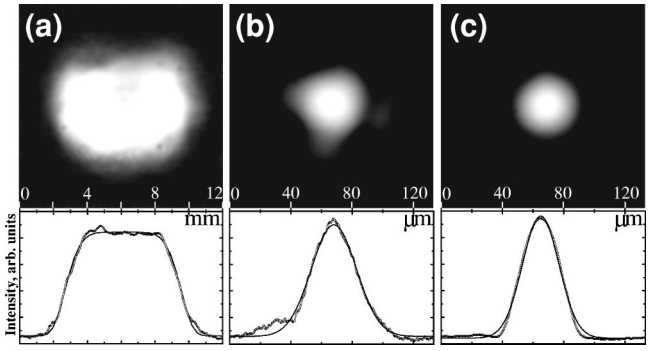

FIG. 6. Spatial beam profiles: (a) unfocused amplified beam, FWHM =6 mm; (b) focused amplified beam ($f=20$ cm), waist=41 μm; (c) focused cw-seeding beam ($f=20$ cm), waist=33 μm.

The chirp shift in the laser system presented here is evaluated by simultaneously measuring the transmission through an etalon of both the seeding cw light and the amplified pulses, while scanning the Ti:Sa ring laser. The etalon (FSR=21 GHz) used is the same one employed to measure the frequency bandwidth of the pulses. Due to the high peak intensity of the pulsed light, the two signals can not be monitored with the same photodetector; a beam splitter is used to divide the beam transmitted through the etalon. One beam is further attenuated and sent to a fast photodiode which, in combination with a boxcar averager, measures the transmitted intensity of the pulses. The intensity of the other beam is monitored with a slow photodiode, whose signal is gated 100 μs before the arrival of the laser pulses, thus measuring only the contribution of the cw light intensity. The frequency shift is measured at each stage of the amplification chain. It is found that the PDA induces a blueshift in the pulses on the order of 80 MHz, and that the amplification processes in the Ti:Sa crystals do not add any significant chirp shift. It has to be noted that these measurements are performed at a wavelength around 780 nm using LDS 765 dye in the PDA. The frequency shift could be different, even in sign, for different wavelength and dyes. However, on-line measurement of the frequency shift using the etalon is feasible, and is implemented in the system.

B. Spatial beam quality

The evaluation of the spatial beam characteristics of the powerful near-infrared pulses is of particular interest in view of their use for high-order harmonic generation. The so-called plateau of the efficiency in high-order harmonic generation in a gas jet is reached for peak intensities above 10^{13} W/cm^2, that can be obtained by focusing with a lens, providing the spatial quality of the pulses is sufficiently good.

The spatial distribution of the laser beam is recorded using a charge coupled device camera (Hitachi VK-M98E). The power of the beam is attenuated with neutral density filters to avoid saturation of the camera. In Fig. 6(a), the beam profile at the output of the Ti:Sa amplifier at full amplification is shown. The beam has an oval shape with horizontal FWHM of 7 mm and vertical one of about 5 mm. The flat top maximum, is an indication of saturation during the

amplification process. By comparing the transversal beam profiles after each amplification stage we conclude that the spatial nonuniformity is induced in the main Ti:Sa amplifier. When focused with a lens of focal length $f=20$ cm, the beam has distinct vertical and horizontal foci separated by ~ 200 μm. The beam spatial distribution at the intermediate position between the vertical and horizontal foci is imaged with an objective, and shown in Fig. 6(b). The spot is quite symmetric with a waist $w_0=41$ μm, at the $1/e^2$ level of the maximum intensity. The calibration of the spatial dimensions is performed using as reference two wires of 50 and 90 μm. In the lower part of Fig. 6(b) a Gaussian fit is performed on the transverse profile of the beam. After integration of the spatial beam profile distribution in the focus, a peak intensity of 5.2×10^{13} W/cm^2 is deduced, for pulses with 225 mJ of energy and 320 ps time duration. In Fig. 6(c) the focal spot of the seed beam is shown for comparison.

To investigate the focusing capabilities of the high-energy pulses, the beam propagation factor M^2 is estimated; M^2 is equal to 1 for a perfect Gaussian beam. When the beam is focused by a lens the M^2 factor can be evaluated, to a good approximation, using the expression $(\pi w_0 w_L)/(\lambda f)$,[19] where w_L is the beam radius at the lens. Assuming $w_L\sim 6$ mm, the M^2 factor of the amplified beam is estimated to be approximately 2.5. Although the focusing capabilities of the present laser beam are worse then that of a perfect Gaussian beam, power densities above 10^{14} W/cm^2 are feasible in case of focusing with lenses of focal lengths shorter than 15 cm. With this characteristic the present laser source is suitable to perform high-order harmonic generation in the plateau region. This investigation is now in progress and will be the subject of a future publication.

ACKNOWLEDGMENTS

This project was carried out with a research grant from the Netherlands Foundation for Research of Matter (FOM). The authors wish to thank R. van Grondelle and B. Gobets (Laser Center VU) for the use of the femtosecond laser and the fluorescence streak camera in the measurements of the dye decay curves, E. J. van Duijn for stimulating discussions and J. Bouma for the valuable technical support. D.N. acknowledges the support of Marie Curie individual fellowship the European Community under Contract No. HPMFCT-2000-00455.

[1] E. Cromwell, T. Trickl, Y. T. Lee, and A. H. Kung, Rev. Sci. Instrum. **60**, 2888 (1989).
[2] K. S. E. Eikema, W. Ubachs, W. Vassen, and W. Hogervorst, Phys. Rev. A **55**, 1866 (1997).
[3] U. Hollenstein, H. Palm, and F. Merkt, Rev. Sci. Instrum. **71**, 4023 (2000).
[4] J. L. Krause, K. J. Schafer, and K. C. Kulander, Phys. Rev. Lett. **68**, 3535 (1992).
[5] X. F. Li, A. L'Huillier, M. Ferray, L. A. Lompré, and G. Mainfray, Phys. Rev. A **39**, 5751 (1989).
[6] C. Spielmann *et al.*, Science **278**, 661 (1997).
[7] P. A. Heimann *et al.*, Rev. Sci. Instrum. **68**, 1945 (1997).
[8] W. Schade, B. Garbe, and V. Helbig, Appl. Opt. **29**, 3950 (1990).
[9] P. P. Yaney, D. A. V. Kliner, P. E. Schrader, and R. L. Farrow, Rev. Sci. Instrum. **71**, 1296 (2000).
[10] C. Lyngå, F. Ossler, T. Metz, and J. Larsson, Appl. Phys. B: Lasers Opt. **B72**, 913 (2001).
[11] P. Cacciani, W. Ubachs, P. C. Hinnen, C. Lyngå, A. L'Huillier, and C. G. Wahlström, Astrophys. J. Lett. **499**, L223 (1998).
[12] S. Schiemann, W. Ubachs, and W. Hogervorst, IEEE J. Quantum Electron. **33**, 358 (1997).
[13] S. Schiemann, W. Hogervorst, and W. Ubachs, IEEE J. Quantum Electron. **34**, 407 (1998).
[14] D. Neshev, I. Velchev, W. Majewski, W. Hogervorst, and W. Ubachs, Appl. Phys. B: Lasers Opt. **B68**, 671 (1999).
[15] I. Velchev, R. van Dierendonck, W. Hogervorst, and W. Ubachs, J. Mol. Spectrosc. **187**, 21 (1998).
[16] H. Knöckel, S. Kremser, B. Bodermann, and E. Tiemann, Z. Phys. D: At., Mol. Clusters **37**, 43 (1996).
[17] M. S. Fee, K. Danzmann, and S. Chu, Phys. Rev. A **45**, 4911 (1992).
[18] N. Melikechi, S. Gangopadhyay, and E. E. Eyler, J. Opt. Soc. Am. B **11**, 2402 (1994).
[19] N. Hodgson and H. Weber, *Optical Resonators* (Springer, London, 1997), pp. 605–608.